

Accepted Manuscript

Inhibition of autophagy by chloroquine potentiates synergistically anti-cancer property of artemisinin by promoting ROS dependent apoptosis

Arnab Ganguli, Diptiman Choudhury, Satabdi Datta, Surela Bhattacharya, Gopal Chakrabarti



PII: S0300-9084(14)00287-9

DOI: [10.1016/j.biochi.2014.10.001](https://doi.org/10.1016/j.biochi.2014.10.001)

Reference: BIOCHI 4557

To appear in: *Biochimie*

Received Date: 19 July 2014

Accepted Date: 1 October 2014

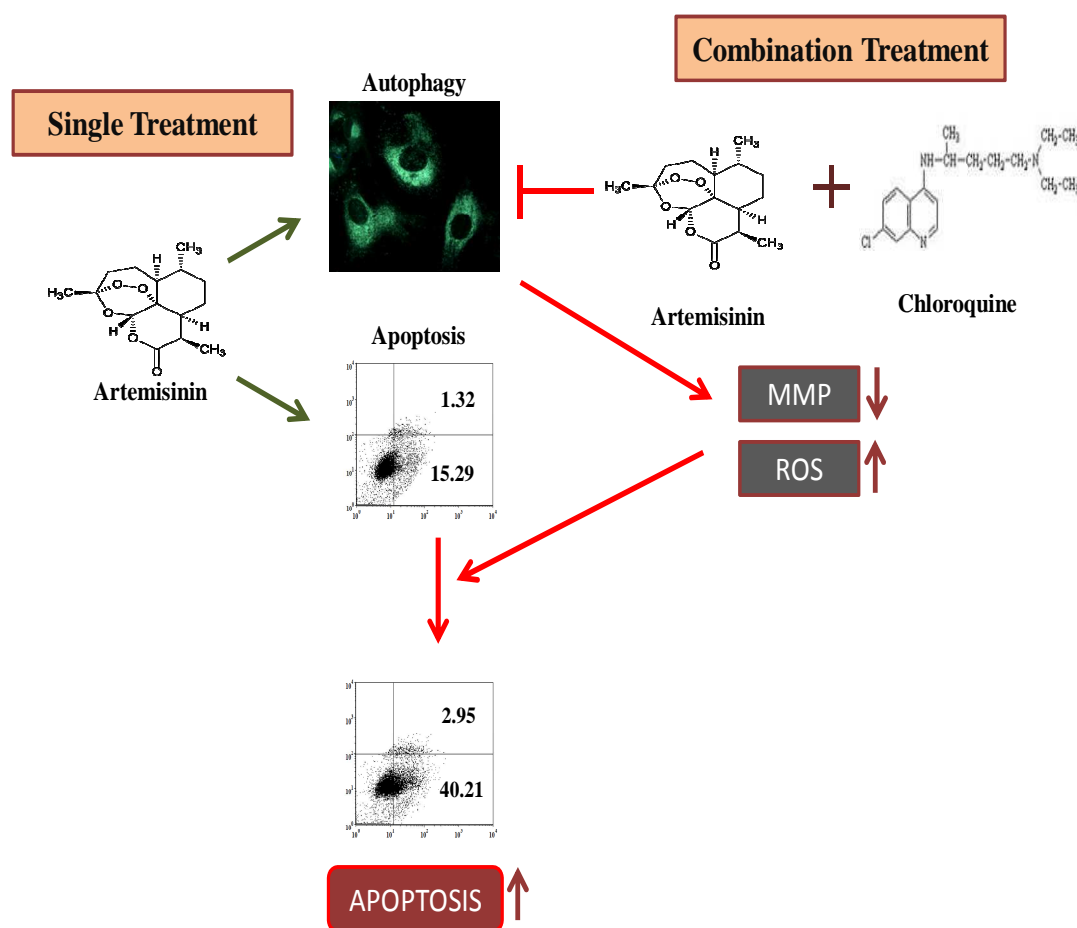
Please cite this article as: A. Ganguli, D. Choudhury, S. Datta, S. Bhattacharya, G. Chakrabarti, Inhibition of autophagy by chloroquine potentiates synergistically anti-cancer property of artemisinin by promoting ROS dependent apoptosis, *Biochimie* (2014), doi: 10.1016/j.biochi.2014.10.001.

This is a PDF file of an unedited manuscript that has been accepted for publication. As a service to our customers we are providing this early version of the manuscript. The manuscript will undergo copyediting, typesetting, and review of the resulting proof before it is published in its final form. Please note that during the production process errors may be discovered which could affect the content, and all legal disclaimers that apply to the journal pertain.

Graphical Abstract:

Inhibition of autophagy by chloroquine potentiates synergistically anti-cancer property of artemisinin by promoting ROS dependent apoptosis.

Arnab Ganguli, Diptiman Choudhury, Satabdi Datta, Surela Bhattacharya and Gopal Chakrabarti*



Inhibition of autophagy by chloroquine potentiates synergistically anti-cancer property of artemisinin by promoting ROS dependent apoptosis.

Arnab Ganguli, Diptiman Choudhury, Satabdi Datta, Surela Bhattacharya and Gopal Chakrabarti*

Department of Biotechnology and Dr. B.C. Guha Centre for Genetic Engineering and Biotechnology, University of Calcutta, 35 Ballygunge Circular Road Kolkata, WB 700019, India.

***Correspondence to:**

Gopal Chakrabarti

Department of Biotechnology and Dr. B.C. Guha Centre for Genetic Engineering and Biotechnology, University of Calcutta

35 Ballygunge Circular Road, Kolkata, West Bengal, India, 700019.

Telephone: +91-33-2461-5445

Fax : +91-33-2461-4849

Email : gcbcg@caluniv.ac.in

Abstract

Artemisinin (ART) is a well-known anti-malarial drug, and recently it is shown prospective to selectively kill cancer cells. But low potency makes it inappropriate for use as an anticancer drug. In this study, we modulated the ART-induced autophagy to increase Potency of ART as an anticancer agent. ART reduced the cell viability and colony forming ability of non-small lung carcinoma (A549) cells and it was non-toxic against normal lung (WI38) cells. ART induced autophagy at the early stage of treatment. Pre-treatment with chloroquine (CQ) and followed by ART treatment had synergistic combination index (CI) for cell death. Inhibition of autophagy by CQ pre-treatment led to accumulation of acidic vacuoles (AVOs) which acquainted with unprocessed damage mitochondria that subsequently promoted ROS generation, and resulted releases of Cyt C in cytosol that caused caspase-3 dependent apoptosis cell death in ART-treated A549 cells. Scavenging of ROS by antioxidant N-acetyl-cystein (NAC) inhibited caspase-3 activity and rescued the cells from apoptosis. Similar effects were observed in other cancer cells SCC25 and MDA-MB-231. The appropriate manipulation of autophagy by using CQ provides a powerful strategy to increase the Potency of selective anticancer property of ART.

Keywords Artemisinin; Chloroquine; Anticancer agent; Autophagy; Apoptosis

Abbreviations

ART, Artemisinin; CQ, Chloroquine; PI, Propidium iodide; MTT, (3-(4,5-dimethylthiazolyl-2)-2, 5-diphenyltetrazolium bromide); AO, Acridine orange; MDC, Monodansylcadaverin; EB, Ethidium bromide; AVOs, Acidic vacuoles; ROS, Reactive oxygen species; MMP, mitochondrial membrane potential change:

1. Introduction

Artemisinin (ART) is a sesquiterpene lactone isolated from the sweet wormwood *Artemisia annua L.*, usually use as an anti-malarial drug [1]. Recently, ART is also emerging as an anticancer agent and studies show that ART is more cytotoxic to cancer cells than normal cells [2, 3]. It is due to the fact that the metabolic activity and cell divisions in cancer cells are more rapid than normal cells. Therefore, compare to normal cells, cancer cells uptake more iron from environment through transferrin receptor. This iron activates the endoperoxide linkage of ART leading to generation of highly cytotoxic carbon centred radical or reactive oxygen species which is similar of its cytotoxic action against malaria [4, 5]. Therefore, ART not only shows toxicity against cancer cells, but also its toxicity selectivity towards cancer cells makes ART as a promising anticancer agent. Several different molecular mechanisms of anticancer activity of ART have been investigated. Apoptosis has been commonly reported mechanism of its cytotoxic action [6-8], beside this, induction of autophagy [9], cell cycle arrest [10], ROS generation [7], involvement of iron [3, 10, 11] also been demonstrated well in ART induce cytotoxicity in cancer cells. However, the low toxicity and low bio-availability make it unsuitable for use as an anticancer agent. Works are going on to try to increase the potency of artemisinin and make it acceptable as an anticancer drug.

Autophagy is a cellular event, induced by several extracellular stressor or internal needs, where many cytosolic materials like organelles and several proteins are accumulated in a double layer membrane vesicle called autophagosomes then it is fused with lysosomes where internal materials are degraded [12, 13]. The roles of autophagy in cancer cells are not so clear. Some reports which demonstrate that autophagy act as a protective mechanism in 5FU [14], sulforaphane [15], imatinib [16] induce cancer cell death. Whereas under certain circumstances excessive or unquenched autophagy leads to cell death called programme cell death type II (PCDII), this is characteristically differ from apoptosis [17, 18]. So as evidently

the autophagy in cancer cells may depend on the kind of tumour, stimuli and also phases of tumorigenesis. If we would try to modulates autophagy induced by anticancer agents in an appropriate manner that may increase its potency against cancer cells.

To increase the potency of anticancer agents by inhibiting autophagy, different autophagy inhibitors have been used [19, 20]. Interestingly, some previous reports suggest that inhibition of autophagy at a late stage can effectively increase cytotoxicity of anticancer agents towards cancer [16, 21, 22]. One of the well known late phase autophagy inhibitor is chloroquine (CQ). For more than six decades CQ has been using to treat several diseases (like, malaria, rheumatoid arthritis, lupus) because of its high effectiveness and well tolerated by human [23]. Recently, it is also found to be effective against cancer [24, 25]. CQ is a weak base that is readily distributed in human body when it is administered. At cellular levels its unprotonated form can diffuse through the plasma membrane, and its protonated forms are trapped within the acidic vacuoles (late endosome and lysosome), causing increased in pH, inactive lysosomal hydrolysates, thus increase the autolysosomes accumulation by inhibiting the autophagy. This function has been found useful in potentiating the killing effect of radiated cancer cells and other chemotherapeutic agents like 5FU [20], AKT inhibitors [26], src kinase inhibitors such as saracatinib [27].

In the present study, we were interested to investigate ART induced autophagy and selective apoptosis in A549 cells. Next we would like to examine whether the clinical potency of ART would be increased when it was treated along with CQ. Results of this report demonstrated that indeed potency of anticancer activity of ART was increased in the presence of CQ which could be a promising strategy for application of ART for treatment of cancer in future.

2. Material and Methods

2.1. Materials

Artemisinin, DAPI, mice monoclonal antihuman alpha tubulin primary antibody, FITC conjugated antihuman α -tubulin antibody, TRITC conjugated goat monoclonal antimouse IgG, goat monoclonal antirabbit IgG antibody TRITC conjugated, mouse monoclonal IgG anti human antibodies (Beclin I, LC3, p62, Bax, Bcl-2, caspase-3, Cyt C, β -actin), HRP conjugated goat monoclonal antimouse IgG antibody, RNase-A, PI, DMSO were purchased from SIGMA, USA. Ham's F12 nutrient media and DMEM nutrient media (supplemented with 1mM L-glutamine), Bovine Fetal Serum, Penicillin- streptomycin mixture, 100 mM Fungizone (Amphotericin B) and hydrocortisone were purchased from HyClone, USA. Trypsin-EDTA was purchased from Hi Media, India. Anti-mouse HRP conjugated secondary antibody, Bradford Protein estimation kit were purchased from GeNei, India. RIPA buffer was purchased from PIERCE, USA. chemiluminescence substrate was purchased from Thermo, USA, and other chemicals were of analytical grade and were purchased from Sisco Research Laboratory, India.

2.2. Maintenance of Cell Culture

Human lung carcinoma (A549) cells were maintained in Ham's F12 nutrient media, human normal lung fibroblast (WI38) cells and human breast cancer (MDA-MB-231) cells were maintained in DMEM nutrient media and human oral carcinoma (SCC25) cells were maintained in Ham's F12 nutrient media and DMEM nutrient media (1:1 ratio) supplemented with 400 ng/ml hydrocortisone, 2.5 mM L-glutamine, and all these media were additionally supplemented with 1mM L-glutamine, 10% fetal bovine serum, 0.2% NaHCO_3 , 1 mM penicillin, 1 mM streptomycin and 1 mM fungizone (pH 7.4). The cells were cultured at 37 °C maintain humidified atmosphere which containing 5% CO_2 . Cells were grown in

tissue culture flasks until they were become 80% confluent before trypsinization with 1% trypsin-EDTA and splitting.

2.3. Cytotoxicity assay

By using MTT (3-(4,5-dimethyl thiazolyl-2)-2,5-diphenyltetrazolium bromide) assay we measured cytotoxicity induced by ligands in different cells. At first, cells were plated in 96-well culture plates (1×10^4 cells per well). After 36 h incubation, the cells were treated with ligands for required time. MTT (5 mg/ml) was dissolved in PBS and filter sterilized, then 20 μ l of the prepared solution was added to each well and cells were incubated until a purple precipitate was visible. Then 100 μ l of triton-X was added and left the well in the dark for 2 h at room temperature. The absorbance was measured on an ELISA reader at a test wavelength of 570 nm and a reference wavelength of 650 nm. Percentage of cell viability was calculated by the following formula:

$$\% \text{ inhibition} = (100 - (A_t / A_s) \times 100) \times \%$$

A_t and A_s indicated the absorbance of the test substances and solvent control, respectively.[28, 29]

2.4. Colony Forming Assay

Cells were seeded into 35 mm plates. After 24 h culture, cells were treated in the presence or absence of ligands . After treatment, cells were detached from plates by using trypsin-EDTA. Then cells were suspended in fresh culture medium and those were plated 200 cells/well in to 24-well microtiter plates and allowed to grow for 14 days under normal cultural condition (37°C, 5% CO₂). After 14 days, media were removed from wells and washed with PBS, fixed with 4% para-formaldehyde then 0.05% crystal violet was added and incubated for 30 min to

stained colony. Samples were washed with water and finally measured OD at 540 nm after solubilising crystal violet in methanol [20].

2.5. Cell cycle phase distribution analysis

Effect of ligands on cell cycle progression of A549 cells were monitored by flow cytometer using BD FACSCalibur instrument and analyzed by FCS Express software. The cell cycle distribution patterns were determined after processing of treated cells with RNase A followed by staining with PI [28, 29].

2.6. Estimation of apoptotic cells

Apoptosis was measured with an annexin V-FITC apoptosis detection kit. Cultured A549 cells (1×10^5) were incubated with different ligands for 72 h. Approximately 1×10^5 cells were then stained for 15 min at room temperature in the dark with fluorescein isothiocyanate (FITC)-conjugated annexinV ($1 \mu\text{g/ml}$) and propidium iodide (PI) ($0.5 \mu\text{g/ml}$) in a Ca^{2+} -enriched binding buffer, and analyzed by a two colour flow cytometric assay. Annexin V and PI emissions were detected in the FL1 and FL2 channels of a FACSCalibur (Becton-Dickinson, USA) using emission filters of 525 and 575 nm, respectively. The annexin V-negative/PI-negative population were regarded as normal, healthy cells, while annexin V-positive/PI-negative and annexin V-positive/PI-positive were taken as a measure of early apoptosis and late apoptosis, respectively. The data were analysed using FCS Express software [28, 29].

2.7. Detection and quantification of AVOs by acridine Orange (AO) and monodansylcadaverine (MDC)

Acridine orange stain acidic vacuoles by appearance of red fluorescence and when it is localized in cytoplasm and nucleus, then it appears as green. Monodansyl cadaverin (MDC) selectively labels autophagic vacuoles. Therefore, we used these two probes separately to stain AVOs. For fluorescence microscopic of imaging of AVOs, cells were seeded on cover slip at 35 mm plates and incubated in the presence and absence of ligands. After treatment, cells were washed with PBS, then acridine orange (1 μ g/ml), or monodansylcadaverin (50 μ M) was added and incubated for 15 and 10 min respectively. After incubation, cells were washed with PBS, mounted into slides and images were taken by fluorescence microscope [30].

For quantification of AVOs by flow cytometric method, cells were treated with or without ligands. After the treatment, cells were removed from plates by trypsin-EDTA. After washing with PBS, samples were incubated with acridine orange (1 μ g/ml) for 15 min and samples were analyzed using the FACScan flow cytometer and FCS Express software [30].

2.8. Detection of Mitochondrial Membrane Potential (MMP) by JC 1 staining

Mitochondrial membrane potential changes were detected using the fluorescent probe JC-1 (Sigma, USA), a lipophilic cationic dye which accumulates in the living mitochondria. At low MMP, the dye exists as a monomer and emits green fluorescence, but with the increase in the MMP, JC-1 forms J-aggregates. Dye aggregation leads to a shift in fluorescence emission from green to red. For flow cytometric analysis, treated A549 cells were incubated for 15 min with 1 μ g/mL JC-1 in culture medium at 37 °C. Green fluorescence and red fluorescence were detected by FL-1 and FL-2 filters, respectively, using Becton Dickinson FACSCalibur and then analyzed by FCS Express software [29, 30].

2.9. Detection of ROS Generation by DCF-DA staining

ROS generation was determined by DCF-DA staining using flow cytometer. Briefly, A549 cells (1×10^5) in DMEM media were treated with ligands for 72 h, treated cells were detached with trypsin-EDTA, and washed twice with PBS. To assess the ROS generation cells were re-suspended in 0.5 ml PBS containing $10 \mu\text{M}$ DCF-DA (sigma) for 15 min. Cells were then subjected to Becton Dickinson FACSCalibur for flow-cytometric assay and data was analyzed by FCS Express software [29, 31].

2.10. Western blot analysis

After ligand treatment, cells extract were prepared by using RIPA buffer. Western blot for different cellular pathways like apoptosis or autophagy regulatory proteins (p53, Bcl-2, bax, caspase 3, Cyt C, LC3 II, and Beclin I) of treated cells were performed. Primary antibodies dilutions were done according to manufacturer's instruction. β -actin was used for loading controls [30]. The protein concentration was estimated by the method of Bradford [32].

2.11. Statistical Analysis

Data are presented as the mean of at least three independent experiments along with standard error of the mean (SEM). Statistical analysis of data was done by one-way analysis of variance (ANOVA), with Student–Newman–Keul test by using Sigma plot 11.0. The P value <0.05 was considered to be statistically significant.

3. Results

3.1. Effect of ART on cell viability of A549 and WI38 cell line

The effect of ART on cell viability of non-small-cell lung carcinoma A549 cell line and normal lung WI38 cell line were determined by MTT assay. Cultured both A549 and WI38 cells were treated separately with (0 - 1000 μ M) ART for 48 h and (0 - 250 μ M) ART for 72 h and cell viability of ART-treated A549 and WI30 cells were estimated separately (Fig.1A and B). Results of the experiment showed that dose-dependent increase of cytotoxicity of ART in treated-A549 cells. The calculated IC₅₀ value of ART for lung carcinoma A549 cells was 395.2 ± 6.7 μ M for 48 h and 142.5 ± 5.7 μ M for 72 h treatment. However, very little cytotoxic effect of ART was observed in normal lung (WI38) cell, as we found that nearly 92% and 86% cells were remained viable, when WI38 cells were treated with 1000 μ M ART for 48 h and 250 μ M ART for 72 h.

3.2. Effect of ART on clonogenic survival of A549 cells

We used clonogenic assay to determine antitumor activity of ART. We found that the colony formation ability of A549 cells was decreased in dose-dependent manners. For example, when A549 cells were treated with 150 μ M ART, after 14 days, cells were only able to form 50% colony as compared with vehicle control (Fig.1C and D).

3.3. ART increased sub G1 population in cell cycle distribution and apoptosis in A549 cells

Cell cycle distribution of 72 h ART-treated A549 cells were analysed using flow cytometer. Any specific cell cycle arrest pattern in ART-treated cells was not observed but analysis of data showed that sub-G1 population, which indicates cell death, were increased in a dose-dependent manners (Fig. 2A). About 35 ± 2.9 % and 52 ± 4.1 % population of cells were

present at sub-G1 phase, when cells were treated 100 and 150 μ M ART respectively, whereas in vehicle control cells, only 7 ± 2.3 % cells were present in sub G1 phase (Fig. 2B). Generally hypoploidy SubG1 population represents apoptotic mode of cell death. To confirm the mode of cell death, we used annexin V and propidium iodide double staining flow cytometric method for estimation of population of apoptotic cells in ART-treated A549 cells. At IC_{50} dose (150 μ M), 31.43% cells were found to be early apoptotic and 4% cells were in late apoptotic but in ART-untreated control cells, only 2% early apoptotic populations were found (Fig. 2C). Pretreatment with caspase inhibitor z-VAD-FMK (50 μ M treatment for 2 h) caused reduction of apoptosis in ART-treated A549 cells, which indicating caspase dependent apoptotic mode of cell death. Furthermore, we analyzed expression of pro- and anti-apoptotic proteins in ART treated cells by western blot. We found that anti-apoptotic protein like Bcl-2 was down regulated, whereas pro-apoptotic proteins bax and cleaved caspase-3 were upregulated (Fig. 2D). Therefore, these results indicated that ART induced apoptosis in A549 cells.

3.4. ART treatment induced autophagy in A549 cells

We observed that several stress vacuoles in the A549 cells were appeared after artemisinin treatment (Fig. 3A and B). These vacuoles might arise due to the autophagy induction by artemisinin. To confirm that we used acidic vacuoles indicator acridine orange for observing the autophagy vacuoles using flow cytometry and fluorescence microscopy. Interestingly, in fluorescence microscopic study, huge amount of yellow to red vacuoles were observed in artemisinin-treated A549 cells (Fig. 3C and D). Flow cytometric study also supported the same observation (Fig. 3G and H). Latter for further confirmation of autophagy, we used monodansylcadaverin (MDC) staining that specifically accumulated in mature autophagic vacuoles rather in other early acidic endosomal compartments. MDC staining revealed that

huge amount of green AVOs formation occurred in 150 μ M ART treated cells after 48 h (Fig. 3E and F). Similar results were also found flow cytometric analysis of ART-treated A549 cells when probing with MDC (Fig. 3I and J).

In addition to these, we analysed the status of the expression of autophagic marker proteins like LC3-II, p62 and Beclin I in 48 h ART treated cells by western blot technique. Results of the experiments demonstrated that LC3-II, p62, Beclin I were upregulated in ART-treated cells in a dose- dependent manners (Fig. 3K).

3.5. Time-dependent autophagy and apoptosis induction in ART treated A549 cells

We were interested to examine whether continuous autophagy was caused to induce apoptosis? Time-dependent autophagy and apoptosis were monitored in ART-treated A549 cells. Cultured A549 cells were treated with 150 μ M ART, and autophagy and apoptosis were monitored with time till 72 h. We observed that time-dependent increase of MDC fluorescence in ART-treated A549 cells upto 48 h and then it was decreased at 72 h (Fig. 4A and C). Whereas annexinV/PI positive apoptotic cells were increased continuously in a time-dependent manners upto 72 h (Fig. 4B and D).

We also analysed the expression status of Beclin I (as autophagic marker) and cleaved caspases 3 (as apoptosis marker) in 150 μ M (below IC_{50} value) ART treated cells at different time point. We found that expression of Beclin I was increased up to 48 h and then decreased to basal level after 72 h, however, expression of cleaved caspase 3 level was increased in a time-dependent manners (Fig. 4E).

3.6. Effect of autophagic inhibitors on ART induced cell viability of A549 cells

Earlier reports demonstrated that manipulation of autophagy using late stage autophagy inhibitors increased the potency of anticancer agents [16, 19, 20]. Hence, we used late phase

autophagy inhibitor chloroquine (CQ) and estimated the cell viability of ART treated A549 cells. We used two treatment regimes for CQ to sensitize A549 cells towards ART. For pre-treatment regime, we treated A549 cells with 25-100 μM CQ for 12 h and subsequently after washing the cells, treatment with 75 μM ART for 72 h was performed. For co-treatment, we used 75 μM ART and different concentration of CQ (2.5-25 μM) simultaneously to treat A549 cells for 72 h. In both the cases, we measured cell viability by MTT assay and calculated combination index (CI) (Fig 5A-D). We found that CI value of pre-treatment (Fig. 5A and C) were much more lower than CI values of co-treatment (Fig.5 B and D), indicating pre-treatment had synergistic effect where as co-treatment had nearly an additive effect. Furthermore co-treatment also reduced cell viability of normal cells (Fig. 5E) but pre-treatment did not have any cytotoxic effect towards normal cells (Fig. 5F). These results indicated that pre-treatment regime had better potency than co-treatment regime to increase the anti cancer potency of ART. We selected 50 μM CQ (pre-treatment) and 75 μM ART combination dose for further experiments as combination of these two low doses had better combination index. This would be designated as combination treatment.

3.7. Effect of CQ on ART induced clonogenic survival of A549 cells.

To determine whether CQ pre-treatment potentiates the antitumor activity of ART, we performed clonogenic assay. It is reported that the *in vitro* clonogenic assays correlate very well with *in vivo* assays of tumorigenicity in nude mice [33]. We found that when cells were pre-treated with 50 μM CQ for 12 h and followed by treatment with for 72 h, after 14 days only 25% cells were able to form colonies, whereas in individual treatment with ART (75 μM) and CQ (50 μM), 86% and 78% cells were able to form colonies after 14 days (Fig. 5G and H) respectively, which indicated pre-treatment of CQ potentiated antitumor activity of ART.

3.8 Pre-treatment of CQ enhanced the subG1 population and apoptosis in ART-treated A549 cells

As hypoploidy of cells indicate cell death, we wanted to examine the effect of pre-treatment of CQ on induction of hypoploidy cells by ART analysing sub-G1 phase of the cell cycle. We observed that individual treatment of CQ (50 μ M for 12 h) and ART (75 μ M for 72 h) resulted only 8% and 19% subG1 populations, however, when cells were treated with combination of CQ (pre-treatment with 50 μ M for 12 h) and ART (75 μ M for 72 h), the subG1 population was increased to 54% (Fig. 6A and B).

The mode of cell death was determined by annexin V/PI after combination treatment with CQ and ART (Fig. 7C). In control experiments, when cells were treated with separately CQ (50 μ M for 12 h) and ART (75 μ M for 72 h), and the apoptotic populations were 3% and 16% respectively, but in case of combination treatment, apoptotic population was increased to 40% (Fig. 6C). But caspase inhibitor z-VAD-FMK diminishes this effect.

Furthermore we compared expression of pro and anti apoptotic proteins in individual (CQ and ART) and combination (CQ + ART) treated cells by western blot. We found that anti-apoptotic protein like Bcl-2 was more down regulated whereas pro-apoptotic proteins bax and cleaved caspase-3 were more up-regulated when cells were treated in combination compared to individual treatment (Fig. 6D).

3.9. Pre-treatment of CQ enhances ART induced AVOs formation in A549 cells

CQ is a lysomorphobic agent that inhibits late phase autophagy and thus increases AVOs accumulation in the cytoplasm. Previously, we observed that ART induced AVOs formation in A549 cells (Fig. 3A-J). By flow cytometric analysis, we found that number of AVOs in 75 μ M ART treated cells for 48 h significantly increased when cells were pre-treated with 50 μ M CQ for 12 h and then treated with 75 μ M ART for 48 h (Fig.7A and B). These data

indicated that due to inhibition of autophagy at late phase by CQ, the AVOs were accumulating in ART treated cells.

Moreover, when we monitored time-dependent autophagy by MDC staining in A549 cells after pre-treatment of CQ and followed by ART and we found that autophagy remained incomplete, as AVOs were continuously getting accumulated along the whole time-course of treatment i.e. 72 h (Fig.7C and D).

3.10. Pre-treatment with CQ decreased mitochondrial membrane potential and increased ROS generation in ART treated A549 cells

To examine the effect on mitochondria of ART treated cells after inhibiting autophagy by CQ, we used JC1 staining assay to observe the mitochondrial membrane potential. We found that inhibition of autophagy by CQ significantly decreased mitochondrial membrane potential in ART treated cells, which indicated that accumulation of damage mitochondria (Fig. 7 E). We also observed that levels of cytosolic cytochrome C was increased in combination treatment of CQ and ART (Fig. 7F).

Previous reports suggest that cytotoxic ROS may be generated from damage mitochondria [34]. We found that inhibition of autophagy by CQ pre-treatment significantly increased ROS in ART treated cells, as compared with only ART treatment (Fig. 8A). We used NAC which is a ROS scavenger to investigate the effect of ROS on autophagy induction in both individual and combined treated A549 cells. We observed that NAC significantly reduced AVOs in both single and double treated A549 cells (Fig. 8C). Furthermore, scavenging ROS by NAC decreased the cleaved caspase 3 expression (Fig. 8E) and subsequently blocked apoptotic cells death (Fig. 8D) in both ART (pre-treated) and CQ plus ART-treated A549 cells (Fig.8 C-E), therefore enabling protection to cell viability (Fig. 8B).

3.11. ART induced autophagy in other cell lines

We were interested to extent our study to other cell lines to examine whether ART induced autophagic induction was cell specific or not. Results described in Fig. 9 show that in both oral cancer (SCC25) and breast cancer (MDA-MB-231) cells, treatment with ART increased expression of LC3-II and accumulation of MDC in intracellular puncta and this expression of LC3-II and accumulation of MDC were further increased, when autophagy was inhibited by CQ (Fig.9A, B, E and F). Furthermore, 50 μ M CQ pre-treatment (for 12 h) also decreased the viability of ART treated SCC25 and MDA-MB-231 cells (Fig. 9C and D). In both the cells, combination treatment caused apoptosis mode of cell death as we found that cleaved caspase 3 level was increased in both cells lines in double treatment compared with single treatment (Fig 9E and F). Therefore, all these data suggested that induction of autophagy by ART was not cell specific and also inhibition of this autophagy by CQ sensitized cancer cells towards ART.

4. Discussion

Artemisinin (ART) is a well-known anti-malarial drug [1]. Recently, it gets attention to several researchers because of its target cancer cells and shows anticancer property [2, 3]. But it is not considered as effective against cancer due to its low Potency. In this study, our objective was to increase its effectiveness without changing its selective nature against cancer.

In our study, we demonstrated that ART was selectively cytotoxic to non-small cell lung cancer (A549) cells (Fig. 1A-D) and apoptosis was the mode of cell death in ART-treated A549 cells (Fig. 2 C and D). During the course of ART treatment autophagy process were also induced (Fig. 3A-K) and the time-dependent study indicated that autophagy was increased up to 48 h after ART treatment (Fig 4A and C) and then it was reduced to basal levels, whereas apoptosis was increased in a time-dependent manner till 72 h study (Fig. 4B and D). These data demonstrated that autophagy was a cell-survival in ART-treated cells for initial stage of 48 h of treatment, after that extensive autophagy led to cell death.

Several contradictory views of the role of autophagy in cancer chemotherapy have been reported, where autophagy either promotes or inhibits apoptosis [34, 35]. Here in our study, we observed that autophagy was cell survival at initial stage of ART treatment. The strategy was that if we would inhibit ART-induced autophagy at initial stage, then the Potency of anticancer property could be increased. However, to increase the Potency of anticancer agents by autophagy inhibition depends on the type of cells, extent of damage and also type of autophagy inhibitors [36]. Late phase autophagic inhibitors were more efficient than the early phase autophagy inhibitors [16].

In this study, we used late stage autophagy inhibitor CQ to manipulate ART induced autophagy and apoptosis process in A549 cells. Beside autophagy inhibition property of CQ, it is also being clinically used as a drug for several diseases like malaria. For comparative

study, we used two different treatment regimes and based on combination index, pre-treatment of CQ was found to be more effective to increase the potency of artemisinin than co-treatment (Fig.5A-E). Additionally, pre-treatment in contrast with co-treatment not altered the selective anticancer property of artemisinin. Therefore, we selected pre-treatment regime to study further and we found that CQ pre-treatment effectively sensitized cancer cells towards ART (Fig. 5F) by decreased the cell viability, decreased colony forming ability (Fig. 5G and H) and increased percentage of apoptotic cells (Fig. 6C and D) in combination treated A549 cells.

We further investigated the mechanism of autophagy inhibition by CQ which sensitized ART induced apoptosis in A549 cells. We found inhibition of autolysosome formation of pre-treatment with CQ significantly increased AVOs formation (Fig. 7A and B). This is the pathognomonic features of autophagy inhibition by CQ, and these AVOs were not removed from the cells rather accumulating through, the whole time course of combination treatment (Fig. 7C and D). Consequently the cause of apoptosis in the combination treatment might be due to the interruption of degradation of damage mitochondria within the accumulating AVOs in A549 cells as mitochondrial membrane potential decreased in combination treated A549 cells (Fig. 7E), is similar to earlier reports [37, 38] decrease of mitochondrial membrane potential allows Cyt C to release from mitochondria to cytosol and subsequent initiation of apoptosis occurs.

Moreover, as resembling with earlier reports [39], we found that unprocessed damage mitochondria also might increase ROS generation in combination treated A549 cells (Fig. 8A) and to understand the function of this ROS formation, we used antioxidant NAC. NAC treatment completely inhibited ART induced autophagic process and apoptotic cell death (Fig.8 C-E) and also decreased the cell viability of combination treated A549 cells (Fig. 8B). This observation suggested that induction of ROS was an important criterion in ART induced

apoptotic cell death under suppressed autophagic condition. Now this accumulation of ROS might eventually induce caspase-dependent apoptosis in A549 cells (Fig. 8A and B).

We extended our study to find out whether ART induced autophagy was cell type specific or not, we found that ART induced autophagy in different cell lines (SCC25, MDA-MB-231) and inhibition of this autophagy by CQ sensitized those cancer cells towards ART (Fig. 9A-F). Therefore, our data suggest that CQ is a drug which already in clinical usage and repurposing it as a new adjuvant in selective anticancer therapy with ART would be useful, practical and cost effective.

5. Conclusion

Our data suggest that autophagy is induced by ART along with apoptotic cell death in a variety of cancer cells, and inhibition of this autophagy by late autophagy inhibitors CQ increases ROS dependent apoptotic cell death. So the appropriate manipulation of autophagy by using CQ provides a powerful strategy to increase the Potency of selective anticancer property of ART.

Acknowledgement

The work was supported by grants from the Department of Science and Technology, Govt. of India (No. SR/SO/BB-14/ 2008) and the Department of Biotechnology, Govt. of India (No. BT/PR12889/AGR/36/624/2009) to G.C. Confocal Microscope and FACS facilities are developed by the grant from the National Common Minimum Program, Govt. of India. A.G. was supported by a fellowship from the Department of Science and Technology, Govt. of India and Department of Biotechnology, Govt. of India - IPLS . D.C. was supported with a fellowship by CSIR, Govt. of India. We wish to thanks Dr. Atanu Maity, Ramalingaswami Fellow of Department of Biotechnology, Govt. of India, is working our Department, for critical reading of the manuscript.

References

- [1] S.R. Meshnick, Artemisinin: mechanisms of action, resistance and toxicity, *Int J Parasitol*, 32 (2002) 1655-1660.
- [2] H. Lai, N.P. Singh, Selective cancer cell cytotoxicity from exposure to dihydroartemisinin and holotransferrin, *Cancer Lett*, 91 (1995) 41-46.

- [3] N.P. Singh, H. Lai, Selective toxicity of dihydroartemisinin and holotransferrin toward human breast cancer cells, *Life Sci*, 70 (2001) 49-56.
- [4] P.L. Olliaro, R.K. Haynes, B. Meunier, Y. Yuthavong, Possible modes of action of the artemisinin-type compounds, *Trends Parasitol*, 17 (2001) 122-126.
- [5] S.R. Meshnick, A. Thomas, A. Ranz, C.M. Xu, H.Z. Pan, Artemisinin (qinghaosu): the role of intracellular hemin in its mechanism of antimalarial action, *Mol Biochem Parasitol*, 49 (1991) 181-189.
- [6] T. Chen, M. Li, R. Zhang, H. Wang, Dihydroartemisinin induces apoptosis and sensitizes human ovarian cancer cells to carboplatin therapy, *J Cell Mol Med*, 13 (2009) 1358-1370.
- [7] A. Hamacher-Brady, H.A. Stein, S. Turschner, I. Toegel, R. Mora, N. Jennewein, T. Efferth, R. Eils, N.R. Brady, Artesunate activates mitochondrial apoptosis in breast cancer cells via iron-catalyzed lysosomal reactive oxygen species production, *J Biol Chem*, 286 (2011) 6587-6601.
- [8] W. Gao, F. Xiao, X. Wang, T. Chen, Artemisinin induces A549 cell apoptosis dominantly via a reactive oxygen species-mediated amplification activation loop among caspase-9, -8 and -3, *Apoptosis*, 18 (2013) 1201-1213.
- [9] Z. Wang, W. Hu, J.L. Zhang, X.H. Wu, H.J. Zhou, Dihydroartemisinin induces autophagy and inhibits the growth of iron-loaded human myeloid leukemia K562 cells via ROS toxicity, *FEBS Open Bio*, 2 (2012) 103-112.
- [10] Z. Jiang, J. Chai, H.H. Chuang, S. Li, T. Wang, Y. Cheng, W. Chen, D. Zhou, Artesunate induces G0/G1 cell cycle arrest and iron-mediated mitochondrial apoptosis in A431 human epidermoid carcinoma cells, *Anticancer Drugs*, 23 (2012) 606-613.
- [11] R. Handrick, T. Ontikatze, K.D. Bauer, F. Freier, A. Rubel, J. Durig, C. Belka, V. Jendrossek, Dihydroartemisinin induces apoptosis by a Bak-dependent intrinsic pathway, *Mol Cancer Ther*, 9 (2010) 2497-2510.

- [12] B. Levine, J. Yuan, Autophagy in cell death: an innocent convict?, *J Clin Invest*, 115 (2005) 2679-2688.
- [13] M. Katayama, T. Kawaguchi, M.S. Berger, R.O. Pieper, DNA damaging agent-induced autophagy produces a cytoprotective adenosine triphosphate surge in malignant glioma cells, *Cell Death Differ*, 14 (2007) 548-558.
- [14] J. Li, N. Hou, A. Faried, S. Tsutsumi, H. Kuwano, Inhibition of autophagy augments 5-fluorouracil chemotherapy in human colon cancer in vitro and in vivo model, *Eur J Cancer*, 46 (2010) 1900-1909.
- [15] A. Herman-Antosiewicz, D.E. Johnson, S.V. Singh, Sulforaphane causes autophagy to inhibit release of cytochrome C and apoptosis in human prostate cancer cells, *Cancer Res*, 66 (2006) 5828-5835.
- [16] T. Shingu, K. Fujiwara, O. Bogler, Y. Akiyama, K. Moritake, N. Shinjima, Y. Tamada, T. Yokoyama, S. Kondo, Inhibition of autophagy at a late stage enhances imatinib-induced cytotoxicity in human malignant glioma cells, *Int J Cancer*, 124 (2009) 1060-1071.
- [17] M.C. Maiuri, E. Zalckvar, A. Kimchi, G. Kroemer, Self-eating and self-killing: crosstalk between autophagy and apoptosis, *Nat Rev Mol Cell Biol*, 8 (2007) 741-752.
- [18] A. Eisenberg-Lerner, A. Kimchi, The paradox of autophagy and its implication in cancer etiology and therapy, *Apoptosis*, 14 (2009) 376-391.
- [19] J. Li, N. Hou, A. Faried, S. Tsutsumi, T. Takeuchi, H. Kuwano, Inhibition of autophagy by 3-MA enhances the effect of 5-FU-induced apoptosis in colon cancer cells, *Ann Surg Oncol*, 16 (2009) 761-771.
- [20] K. Sasaki, N.H. Tsuno, E. Sunami, G. Tsurita, K. Kawai, Y. Okaji, T. Nishikawa, Y. Shuno, K. Hongo, M. Hiyoshi, M. Kaneko, J. Kitayama, K. Takahashi, H. Nagawa, Chloroquine potentiates the anti-cancer effect of 5-fluorouracil on colon cancer cells, *BMC Cancer*, 10 (2010) 370.

- [21] T. Kanzawa, I.M. Germano, T. Komata, H. Ito, Y. Kondo, S. Kondo, Role of autophagy in temozolomide-induced cytotoxicity for malignant glioma cells, *Cell Death Differ*, 11 (2004) 448-457.
- [22] T. Kanzawa, Y. Kondo, H. Ito, S. Kondo, I. Germano, Induction of autophagic cell death in malignant glioma cells by arsenic trioxide, *Cancer Res*, 63 (2003) 2103-2108.
- [23] V.R. Solomon, H. Lee, Chloroquine and its analogs: a new promise of an old drug for effective and safe cancer therapies, *Eur J Pharmacol*, 625 (2009) 220-233.
- [24] Y. Zheng, Y.L. Zhao, X. Deng, S. Yang, Y. Mao, Z. Li, P. Jiang, X. Zhao, Y. Wei, Chloroquine inhibits colon cancer cell growth in vitro and tumor growth in vivo via induction of apoptosis, *Cancer Invest*, 27 (2009) 286-292.
- [25] C. Fan, W. Wang, B. Zhao, S. Zhang, J. Miao, Chloroquine inhibits cell growth and induces cell death in A549 lung cancer cells, *Bioorg Med Chem*, 14 (2006) 3218-3222.
- [26] C. Hu, V.R. Solomon, G. Ulibarri, H. Lee, The Potency and selectivity of tumor cell killing by Akt inhibitors are substantially increased by chloroquine, *Bioorg Med Chem*, 16 (2008) 7888-7893.
- [27] T. Nishikawa, N.H. Tsuno, Y. Okaji, Y. Shuno, K. Sasaki, K. Hongo, E. Sunami, J. Kitayama, K. Takahashi, H. Nagawa, Inhibition of autophagy potentiates sulforaphane-induced apoptosis in human colon cancer cells, *Ann Surg Oncol*, 17 (2010) 592-602.
- [28] D. Choudhury, A. Ganguli, D.G. Dastidar, B.R. Acharya, A. Das, G. Chakrabarti, Apigenin shows synergistic anticancer activity with curcumin by binding at different sites of tubulin, *Biochimie*, 95 (2013) 1297-1309.
- [29] A. Ganguli, D. Choudhury, G. Chakrabarti, 2,4-Dichlorophenoxyacetic acid induced toxicity in lung cells by disruption of the tubulin-microtubule network, *Toxicology Research*, 3 (2014) 118-130.

- [30] B.R. Acharya, S. Bhattacharyya, D. Choudhury, G. Chakrabarti, The microtubule depolymerizing agent naphthazarin induces both apoptosis and autophagy in A549 lung cancer cells, *Apoptosis*, 16 (2011) 924-939.
- [31] A. Das, S. Chakrabarty, D. Choudhury, G. Chakrabarti, 1,4-Benzoquinone (PBQ) induced toxicity in lung epithelial cells is mediated by the disruption of the microtubule network and activation of caspase-3, *Chem Res Toxicol*, 23 (2010) 1054-1066.
- [32] M.M. Bradford, A rapid and sensitive method for the quantitation of microgram quantities of protein utilizing the principle of protein-dye binding, *Anal Biochem*, 72 (1976) 248-254.
- [33] V.H. Freedman, S.I. Shin, Cellular tumorigenicity in nude mice: correlation with cell growth in semi-solid medium, *Cell*, 3 (1974) 355-359.
- [34] J.M. Suski, M. Lebiezinska, M. Bonora, P. Pinton, J. Duszynski, M.R. Wieckowski, Relation between mitochondrial membrane potential and ROS formation, *Methods Mol Biol*, 810 (2012) 183-205.
- [35] A. Bommareddy, E.R. Hahm, D. Xiao, A.A. Powolny, A.L. Fisher, Y. Jiang, S.V. Singh, Atg5 regulates phenethyl isothiocyanate-induced autophagic and apoptotic cell death in human prostate cancer cells, *Cancer Res*, 69 (2009) 3704-3712.
- [36] T. Shingu, K. Fujiwara, O. Bogler, Y. Akiyama, K. Moritake, N. Shinjima, Y. Tamada, T. Yokoyama, S. Kondo, Stage-specific effect of inhibition of autophagy on chemotherapy-induced cytotoxicity, *Autophagy*, 5 (2009) 537-539.
- [37] H.I. Lin, Y.J. Lee, B.F. Chen, M.C. Tsai, J.L. Lu, C.J. Chou, G.M. Jow, Involvement of Bcl-2 family, cytochrome c and caspase 3 in induction of apoptosis by beauvericin in human non-small cell lung cancer cells, *Cancer Lett*, 230 (2005) 248-259.

[38] M.A. Gallego, B. Joseph, T.H. Hemstrom, S. Tamiji, L. Mortier, G. Kroemer, P. Formstecher, B. Zhivotovsky, P. Marchetti, Apoptosis-inducing factor determines the chemoresistance of non-small-cell lung carcinomas, *Oncogene*, 23 (2004) 6282-6291.

[39] Y. Chen, E. McMillan-Ward, J. Kong, S.J. Israels, S.B. Gibson, Mitochondrial electron-transport-chain inhibitors of complexes I and II induce autophagic cell death mediated by reactive oxygen species, *J Cell Sci*, 120 (2007) 4155-4166.

Figure Legends

Fig. 1. Effect of ART on cell viability and colony forming ability of A549 cells. (A) The cell viability of A549 and WI38 cell lines after ART treatment (0 μ M - 1000 μ M) for 48 h were determined by MTT assay. (B) The loss of cell viability of A549 and WI38 cell lines after ART (0 - 250 μ M) treatment for 72 h were determined by MTT assay. (C-D) Colony forming ability of A549 cells after ART treatment for 72 h was determined by clonogenic assay. All data are represented as mean \pm SEM (*P < 0.05 with respect to control) and representative of at least three independent experiments.

Fig. 2. Effects of ART on cell cycle progression and induction of apoptosis in A549 cells. Cultured A549 cells (1×10^6 cells/ml) were treated with ART (0–150 μ M) for 72 h. (A) The distribution of the cell cycle was analyzed by flow cytometer. (B) The bar diagrams represents percent of hypoploidy subG1 population were present in different concentration of ART treatment. All data are represented as mean \pm SEM (*P < 0.05). (C) ART (IC₅₀ concentration) was added to the A549 cells and cells were incubated for 72 h. Apoptosis (annexin-V positive and PI negative for early apoptotic and annexin-V and PI both positive for late apoptotic) cells were analyzed by flow cytometer (details are described in the Experimental section). Dot plot representations of annexin-V-FITC-fluorescence (x-axis) vs. PI-fluorescence (y-axis) are displayed. All data are representative of at least three independent experiments. (D) Western blot analysis of different apoptosis regulatory proteins (Bax, Bcl-2, cleaved Caspase 3) to confirm induction of cellular apoptosis due to ART treatment. β -Actin was used as a loading control. All data are representative of at least three independent experiments.

Fig. 3. ART induced autophagy in A549 cells. (A-B) Formation of vacuoles in ART treated A549 cells. Bright field microscopic images of vehicle treated (A) and 150 μ M ART treated (B) A549 cells for 48 h were taken with Olympus inverted microscope model CKX41. The black arrows in panel B indicating vacuole formation in ART-treated A549 cells. (C-D) Fluorescence microscopic images of AVOs formation in (0 -150 μ M) ART-treated cells by acridine orange staining. AVOs were appeared as red. All data are representative of at least three independent experiments. (E-F) Fluorescence microscopic images of AVOs formation in (0 -150 μ M) ART treated cells were probed by MDC. AVOs were appeared as green. All data are representative of at least three independent experiments.

(G) Flow cytometric quantification of AVOs formation in ART treated cells after stained with acridine orange, the red fluorescence of acridine orange was quantified by flow cytometer. All data are representative of at least three independent experiments. (H) Mean fluorescence intensity of red fluorescence of acridine orange was plotted against vehicle control and 150 μ M ART treated cells. All data are represented as mean \pm SEM (*P < 0.05).

(I) Flow cytometric quantification of AVOs formation in ART treated cells after stained with MDC, the green fluorescence of MDC was quantified by flow cytometer. All data are representative of at least three independent experiments. (J) Mean fluorescence intensity of green fluorescence of MDC was plotted against control and 150 μ M ART treated cells. All data are represented as mean \pm SEM (*P < 0.05). (K) Western blot analysis for expression of autophagy marker beclin I, LC3, p62 in different concentration of ART treated A549 cells. β -Actin was used as a loading control. All data are representative of at least three independent experiments.

Fig. 4. Time-dependent autophagy and apoptosis induction by ART in A549 cells. (A) Cultured cells were treated with 150 μ M ART and the status of autophagy was determined by

flow cytometry at different time point after staining the AVOs by MDC. All data are representative of at least three independent experiments. (B) Cells were treated with 150 μM ART and apoptosis were estimated by flow cytometer at different time point by using Annexin-V/PI double staining. All data are representative of at least three independent experiments. (C) Mean fluorescence intensity of green fluorescence of MDC (relative quantification of AVOs) was plotted against different time point of ART treatment. . All data are represented as mean \pm SEM (*P < 0.05). (D) Percent of apoptotic cells was plotted against different time point of 150 μM ART treatment. . All data are represented as mean \pm SEM (*P < 0.05). (E) Western blot analysis of autophagy and apoptosis marker beclin I and cleaved caspases 3 respectively at different time points. β -Actin was used as a loading control. All data are representative of at least three independent experiments.

Fig. 5. Inhibition of ART induced autophagy by CQ increased cell death of A549 cells. (A) Cells were pre-treated different concentration of CQ (0-100 μM) for 12 h, then media was removed, and 75 μM ART was added, incubated for 72 h, cell viability was determined by MTT assay. . All data are represented as mean \pm SEM (*P < 0.05). (B) Cells were co-treated with CQ (0-100 μM) and 75 μM ART for 72 h, MTT assay was performed. (C-D) The pre-treatment CI values (C) and co-treatment CI values (D) of different combinations were calculated by using *calculusyn* software. (E-F) Cell viability of normal WI38 cell line was determined after single CQ pre-treatment and co-treatment, single ART treatment and double treatment of both, by using MTT assay. . All data are represented as mean \pm SEM (*P < 0.05). (G-H) Colony forming ability of single (50 μM CQ pre-treatment for 12 h or 75 μM ART) and double (50 μM CQ pre-treatment for 12 h and then 75 μM ART) treated A549 cells were determined by clonogenic assay. All data are represented as mean \pm SEM (*P < 0.05) and representative of at least three independent experiments.

Fig. 6. Pre-treatment of CQ enhanced subG1 population and apoptosis in ART-treated A549 cells. Cultured A549 cells (1×10^6 cells per mL) were single (50 μ M CQ pre-treatment or 75 μ M ART) and double (50 μ M CQ pre-treatment and then 75 μ M ART) treated for 72 h. (A) the distribution of cell cycle was analyzed by flow cytometry. Data were processed and analyzed by the FCS Express software. (B) The graphs represents percent of hypoploidy subG1 population were present in single and double treatment. . All data are represented as mean \pm SEM (*P < 0.05). (C) Apoptosis (annexin-V positive and PI negative for early apoptotic and annexin-V and PI both positive for late apoptotic) cells were measured by flow cytometry (details are described in the Experimental section). Dot plot representations of annexin-V-FITC-fluorescence (x-axis) vs. PI-fluorescence (y-axis) are displayed. Data were processed and analyzed with the FCS Express (D) Western blot analysis for different apoptosis regulatory proteins (Bax, Bcl-2, cleaved caspase 3) to confirm increment of cellular apoptosis due to double treatment. All data are representative of at least three independent experiments.

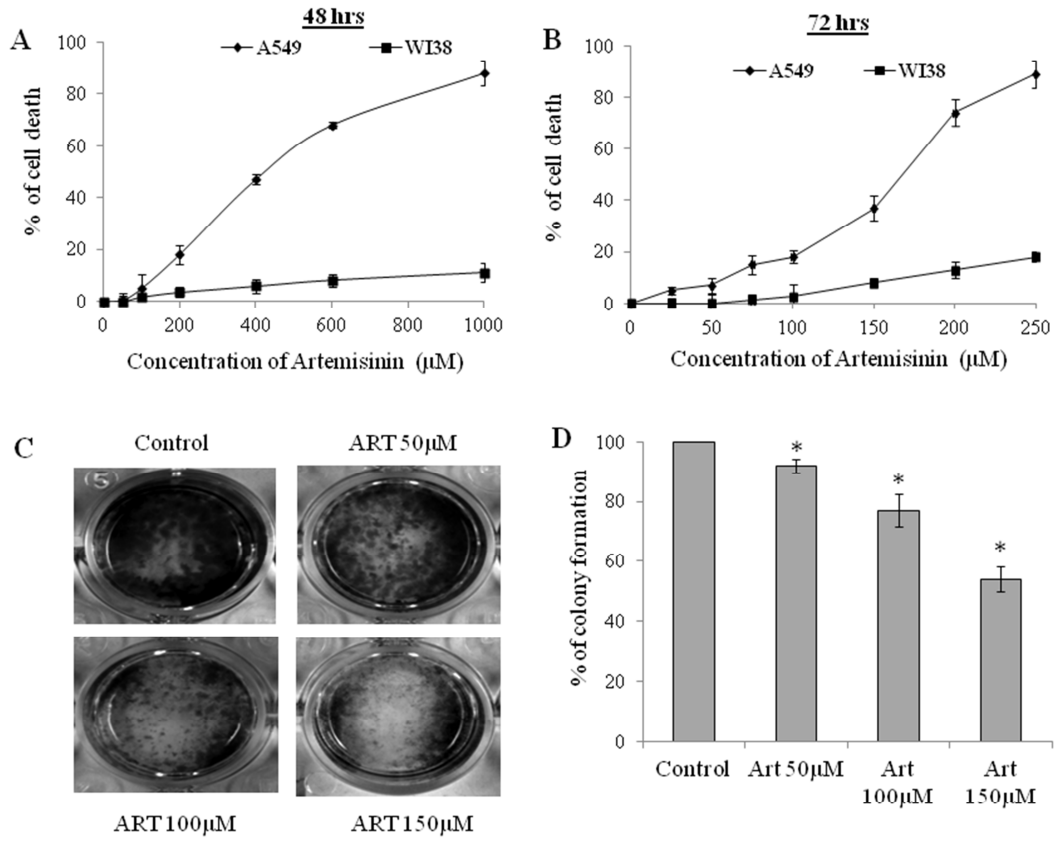
Fig.7. Pre-treatment of CQ caused more accumulation AVOs in ART treated A549 cells. Cultured A549 cells (1×10^6 cells per mL) were separate single (50 μ M CQ treatment for 12 h or 75 μ M ART for 48 h) and double (50 μ M CQ pre-treatment and then 75 μ M ART) treated. (A) Flow cytometric histogram plot of AVOs formation in single and double treated A549 cells by MDC staining. Data were processed and analyzed with the FCS Express software. (B) Mean fluorescence intensity of green fluorescence of MDC was plotted against single and double treatment. Data were processed and analyzed with the FCS Express software All data are represented as mean \pm SEM (*P < 0.05). (C) Flow cytometric histogram plot of AVOs formation in different time point of double treated A549 cells by

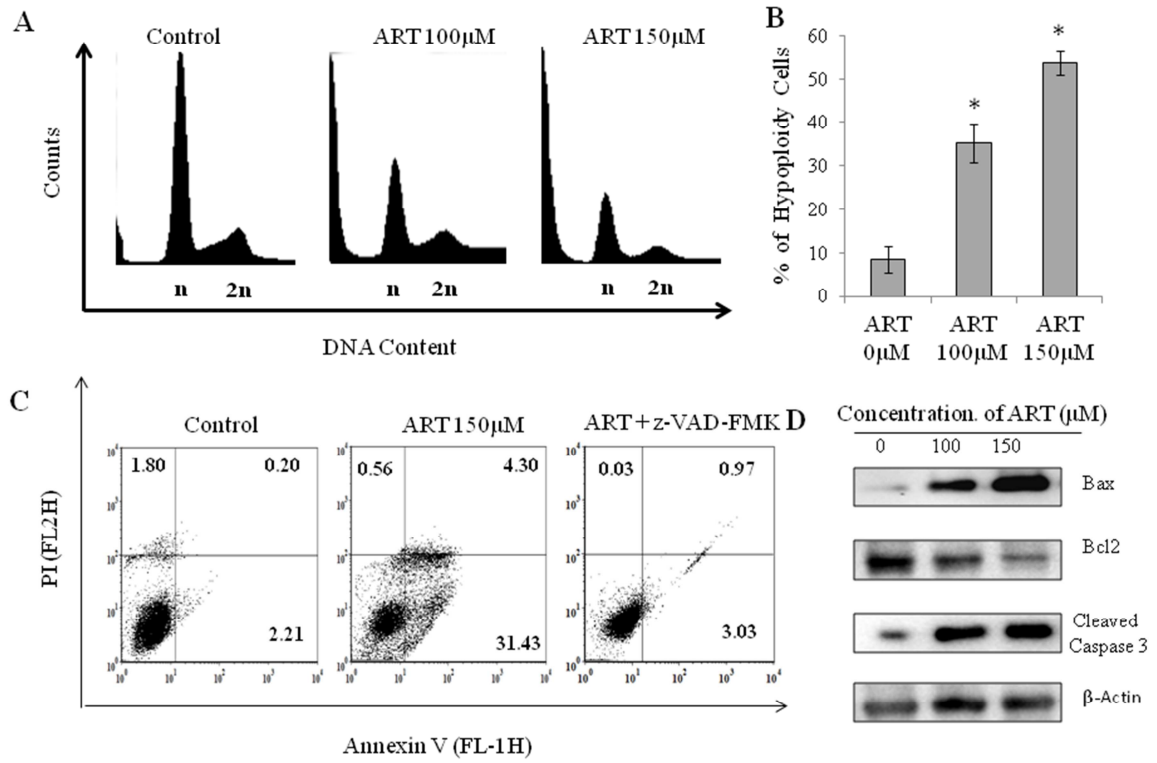
MDC staining. Data were processed and analyzed with the FCS Express software. (D) Mean fluorescence intensity of green fluorescence of MDC was plotted against single and double treatment. Data were processed and analyzed with the FCS Express software. All data are represented as mean \pm SEM (*P < 0.05) and representative of at least three independent experiments. (E-F) Effect of CQ on MMP change and the cytochrome c release by ART treatment. Cultured cells (1×10^6 cells per ml) were single (50 μ M CQ pre-treatment or 75 μ M ART) and double (50 μ M CQ pre-treatment and then 75 μ M ART) treated for 72 h. (E) The effects on mitochondrial membrane potential were determined by using flow cytometry after being stained with JC1 dye. Histogram represents of red fluorescence vs. counts plot. All data are representative of at least three independent experiments. (F) Western blot analysis of cytosolic Cyt C expression due to double treatment. All data representative of at least three independent experiments.

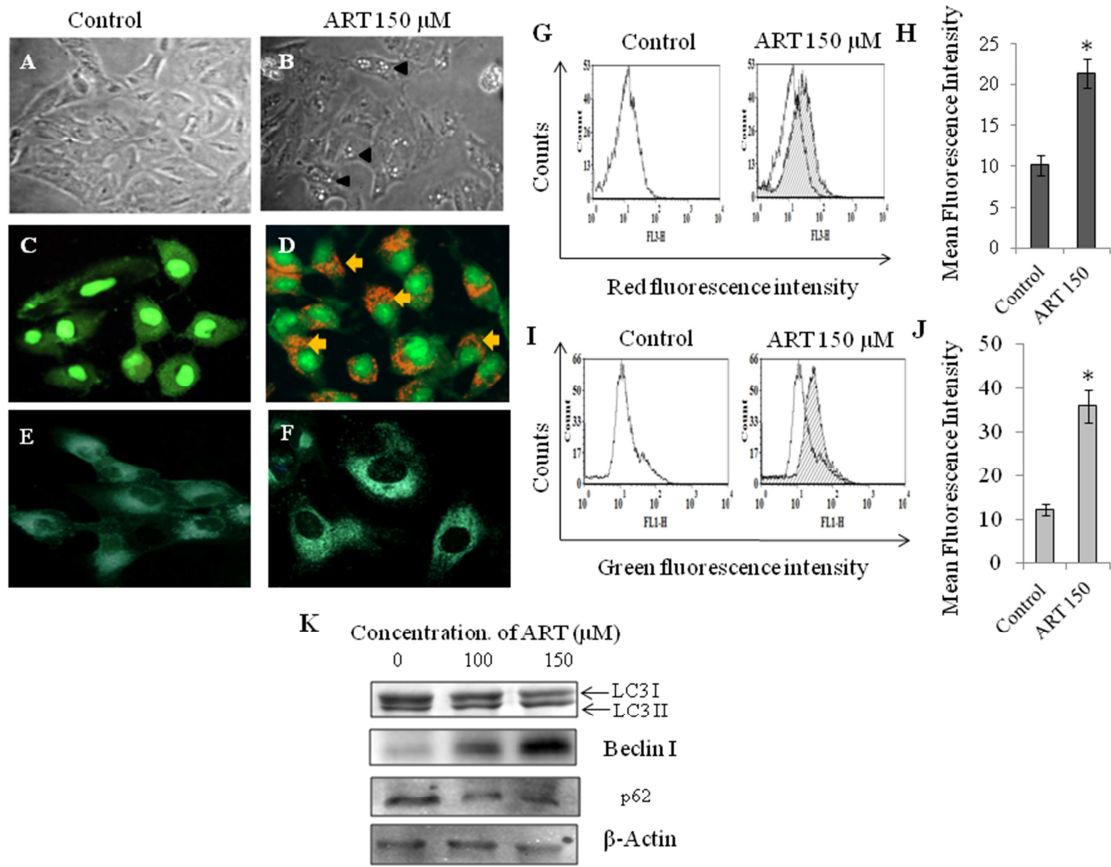
Fig. 8. Pre-treatment of CQ resulted generation of increase level of ROS and induced apoptosis in ART-treated cells. Cells were pre-treated with 10 mM NAC for 1 h prior to 75 μ M ART treatment for 72 h in the presence or absence of 50 μ M CQ pre-treatment. (A) The ROS generation was detected using DCFDA by a flow cytometer. Data were processed and analyzed with the FCS Express software. All data are represented as mean \pm SEM (*P < 0.05). (B) Cell Viability of A549 cells was determined by MTT assay. All data are represented as mean \pm SEM (*P < 0.05). (C) Autophagy was measured by a flow cytometer by using MDC staining. Data were processed and analyzed with the FCS Express software. All data are representative of at least three independent experiments. (D) Apoptosis (annexin-V positive and PI negative for early apoptotic and annexin-V and PI both positive for late apoptotic) cells were measured by flow cytometry (details are described in the Experimental

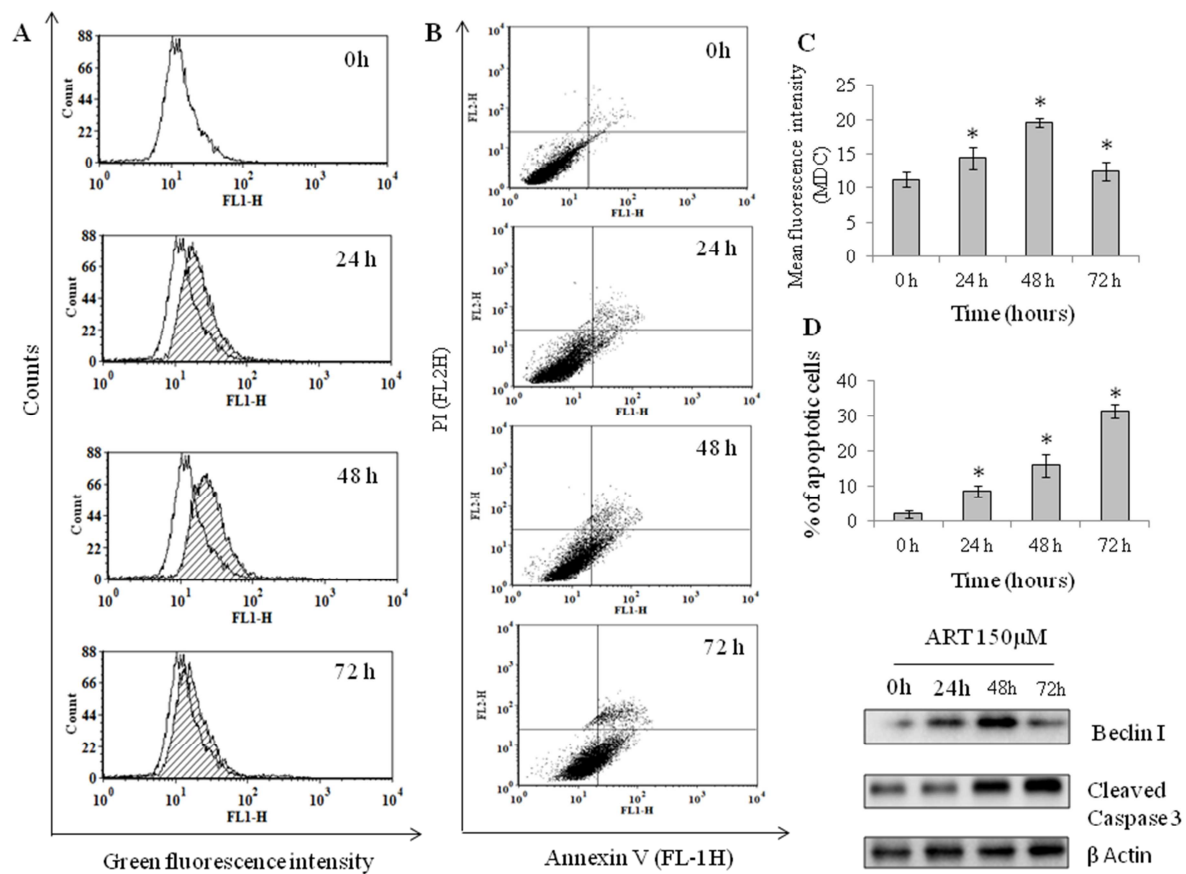
section). Dot plot representations of annexin-V-FITC-fluorescence (x-axis) vs. PI-fluorescence (y-axis) are displayed. All data are representative of at least three independent experiments. (E) The cleave caspase 3 was detected by immunoblotting where β -Actin was used as loading control. Data were processed and analyzed with the FCS Express software. All data are representative of at least three independent experiments.

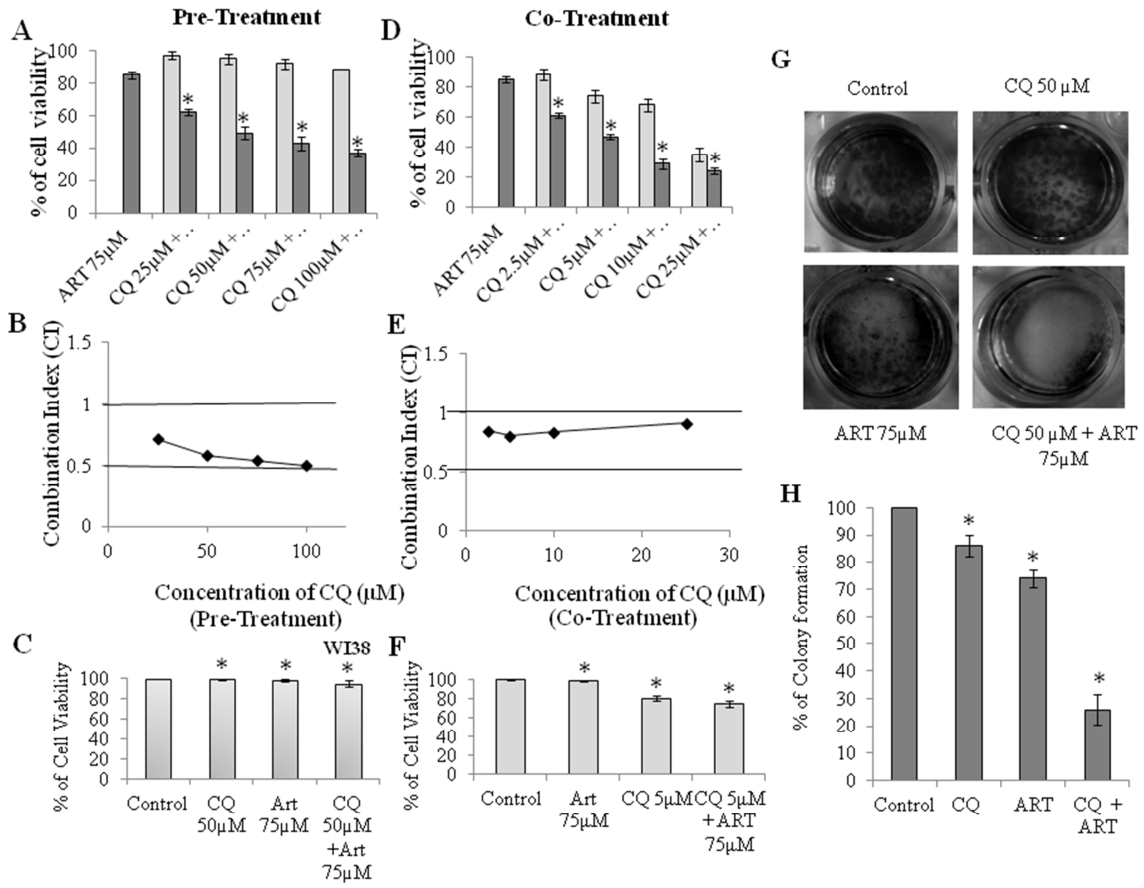
Fig. 9. Inhibition of autophagy by pre-treatment CQ sensitized ART towards other cancer cells. Cultured cells (1×10^6 cells per mL) were single (50 μ M CQ pre-treatment or 75 μ M ART) and double (50 μ M CQ pre-treatment and then 75 μ M ART) treated. (A-B) Fluorescence images of MDC fluorescence of punctuate autophagosome in single and double treated SCC25 (A) MDA-MB-231 (B) were taken after 48 h treatment. All data are representative of at least three independent experiments. (C-D) The cell viability of 0-100 μ M ART treated SCC25 (C) and MDA-MB-231 (D) cells with or without pre-treatment of 50 μ M CQ was determined by MTT assay. All data are represented as mean \pm SEM (*P < 0.05) (E-F) The cleave caspase 3 and LC-III was detected by immunoblotting in single or double treated SCC25 (E) and MDA-MB-231 (F) after 48 h of treatment . All data are representative of at least three independent experiments.

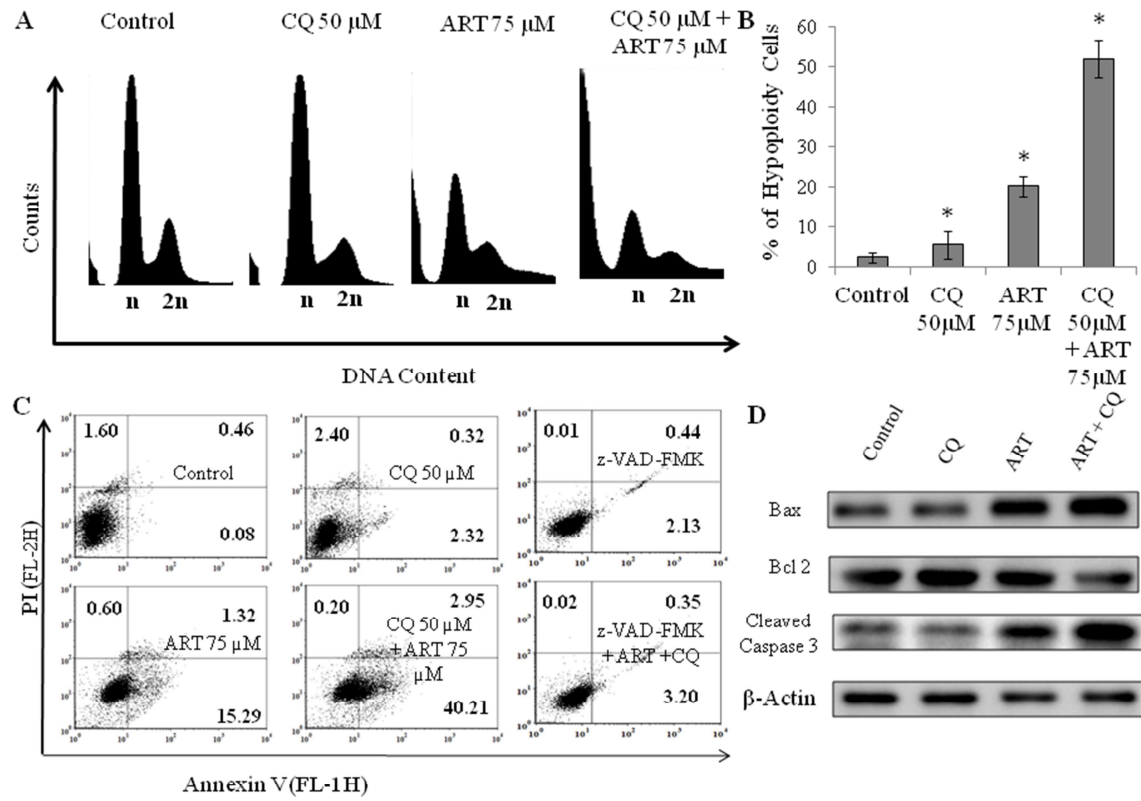


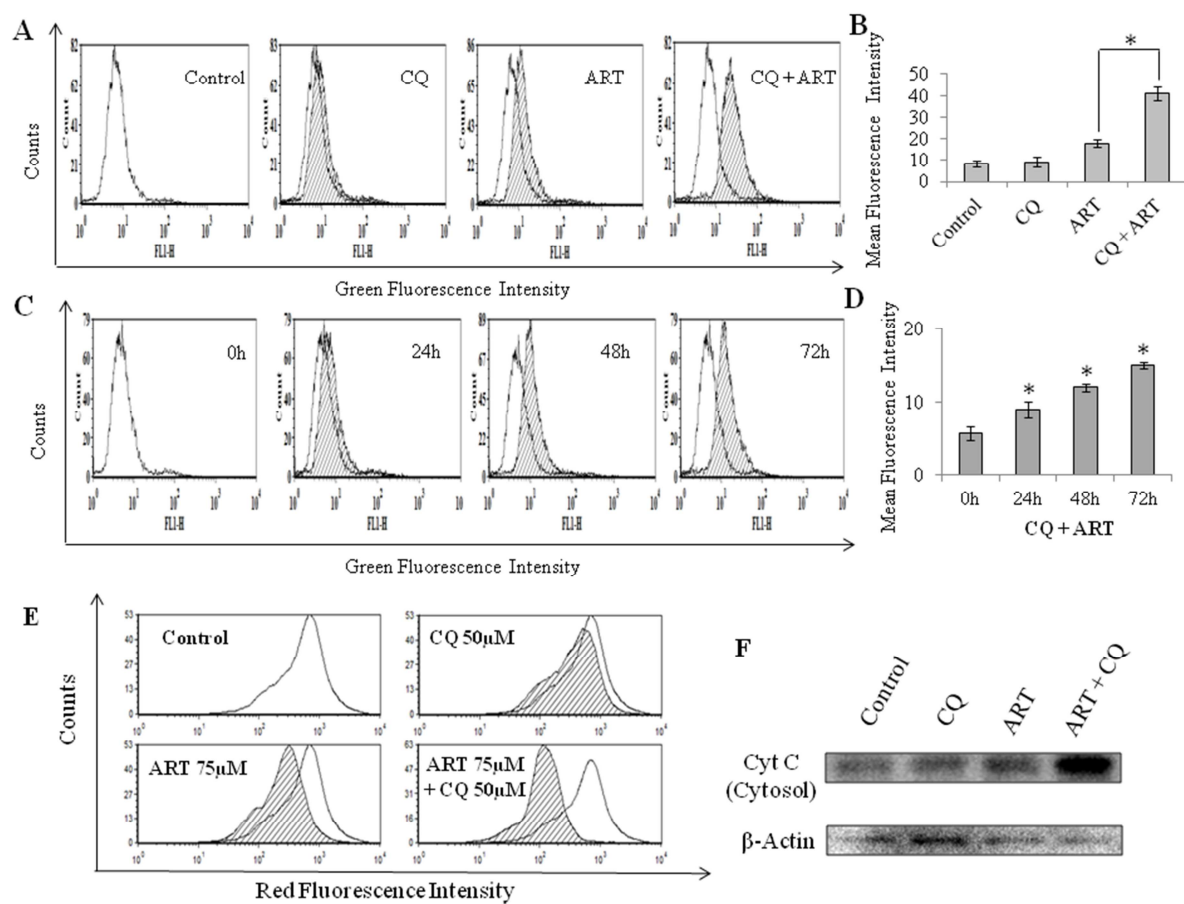


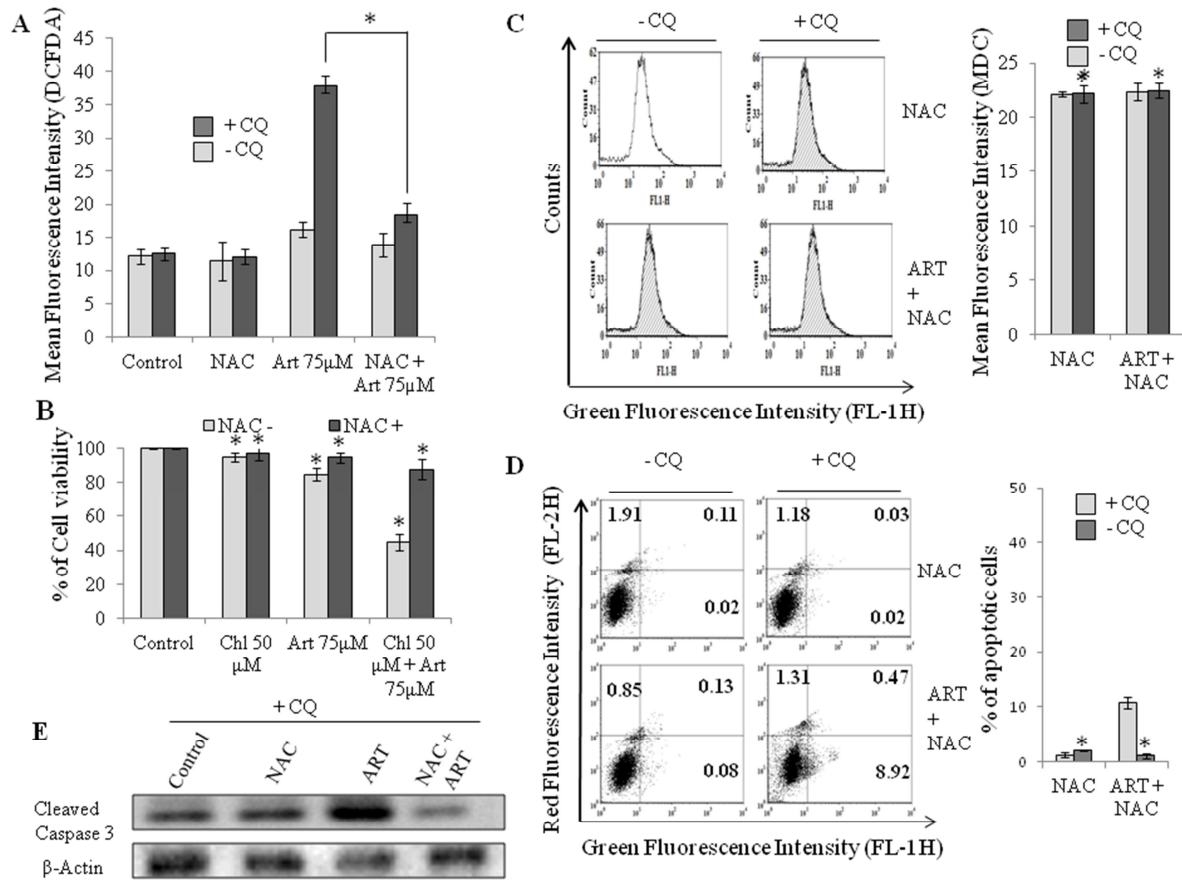


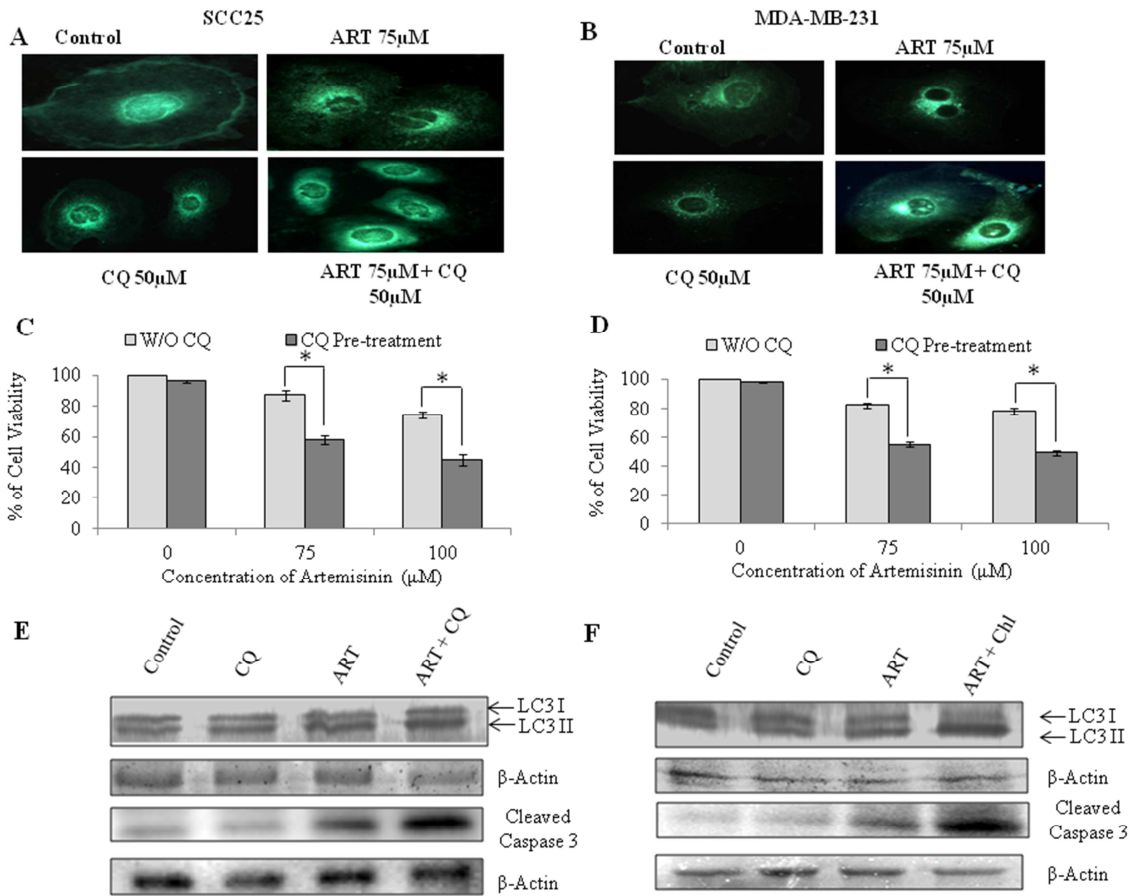












Highlights

- Artemisinin decreased cell viability and colony forming ability of A549 cells but no-toxicity towards normal lung WI38 cells.
- Artemisinin induced autophagy and apoptosis in A549 cells.
- Autophagy inhibition by chloroquine pre-treatment sensitized cell viability of A549 cells towards artemisinin.
- Autophagy inhibition by chloroquine increased AVOs accumulation, decreased MMP and consequently increased ROS.
- Chloroquine pre-treatment also sensitized different cancer cells towards artemisinin.